Cogn Neurodyn (2014) 8:27–35
DOI 10.1007/s11571-013-9266-9

RESEARCH ARTICLE

Visual pattern discrimination by population retinal ganglion cells' activities during natural movie stimulation

Ying-Ying Zhang · Ru-Bin Wang · Xiao-Chuan Pan · Hai-Qing Gong · Pei-Ji Liang

Received: 10 December 2012 / Revised: 21 June 2013 / Accepted: 1 August 2013 / Published online: 14 August 2013

Abstract In the visual system, neurons often fire in synchrony, and it is believed that synchronous activities of group neurons are more efficient than single cell response in transmitting neural signals to down-stream neurons. However, whether dynamic natural stimuli are encoded by dynamic spatiotemporal firing patterns of synchronous group neurons still needs to be investigated. In this paper we recorded the activities of population ganglion cells in bullfrog retina in response to time-varying natural images (natural scene movie) using multi-electrode arrays. In response to some different brief section pairs of the movie, synchronous groups of retinal ganglion cells (RGCs) fired with similar but different spike events. We attempted to discriminate the movie sections based on temporal firing patterns of single cells and spatiotemporal firing patterns of the synchronous groups of RGCs characterized by a measurement of subsequence distribution discrepancy. The discrimination performance was assessed by a classification method based on Support Vector Machines. Our results show that different movie sections of the natural movie elicited reliable dynamic spatiotemporal activity patterns of the synchronous RGCs, which are more efficient in discriminating different movie sections than the temporal patterns of the single cells' spike events. These results suggest that, during natural vision, the down-stream neurons may decode the visual information from the dynamic spatiotemporal patterns of the synchronous group of RGCs' activities.

Keywords Multi-unit recording · Brief movie sections · Population RGCs · MSDD

Electronic supplementary material The online version of this article (doi:10.1007/s11571-013-9266-9) contains supplementary material, which is available to authorized users.

Y.-Y. Zhang · R.-B. Wang · X.-C. Pan
Institute for Cognitive Neurodynamics, East China University Science and Technology, Shanghai 200237, China

H.-Q. Gong · P.-J. Liang (✉)
School of Biomedical Engineering, Shanghai Jiao Tong University, Shanghai 200240, China
e-mail: zhangyyzc@gmail.com

Introduction

An essential goal of the visual neuroscience is to understand the visual information processing in the visual system. Traditionally, investigations toward this goal have been performed using simple and static stimuli and much progress has been achieved (for a review, see Rust and Movshon 2005). However in natural vision, the visual system is facing to complex and dynamic natural stimuli, which are very different from the simple stimuli (Reinagel 2001; Carandini et al. 2005; Felsen and Dan 2005; Geisler 2008). In recent years, naturalistic visual stimuli have been increasingly used in the visual system (Lesica et al. 2008; Mante et al. 2008; Endeman and Kamermans 2010; Talebi and Baker 2012), and it has been demonstrated that the neuronal responses to natural input are not results of superposition of simple constituents (Einhauser and Konig 2010). Thus it is desirable to investigate the information processing of the visual system in response to natural stimuli.

The nervous system conveys sensory information by sequences of spikes (action potentials) of neuronal populations (Rieke et al. 1997; Du et al. 2012). The spike sequences elicited by different stimuli show various spatial and temporal patterns, which are believed to represent the information of the stimuli. Especially, adjacent RGCs often generate concerted spiking activities and more than 50 % spikes of retinal ganglion cells are involved in correlated

and synchronized activities (Brivanlou et al. 1998). The precisely synchronized activities between the neighboring ganglion cells is characterized by a sharp peak with a couple of milliseconds width around zero-lag in the cross-correlogram and they are considered to be mediated by gap junctions between ganglion cells (Brivanlou et al. 1998).Theoretical and experimental studies suggested that synchronized spiking in the retina could carry more information than single cell activities (Meister 1996; Schnitzer and Meister 2003; Schneidman et al. 2006; Pillow et al. 2008; Gong et al. 2010), and thus play an important role in processing and transmitting information (Shlens et al. 2006; Shlens et al. 2009). However, it still remains elusive that whether and how the synchronous RGCs play roles in dynamic natural stimuli discrimination. Traditional methods related to the concerted neuronal activities usually focused on assessment of the synchronization between pair-wise spike trains (Meister et al. 1995; konig 1994; Kreuz et al. 2007). But those methods were unable to deal with population activities involving more than two neurons. While some algorithms have been proposed to detect multi-neuronal synchronous activities, they are restricted to the selection of parameters (Gerstein and Aertsen 1985; Schnitzer and Meister 2003). To illustrate the spatiotemporal patterns of the multiple spike trains, a measurement based on subsequence distribution discrepancy (MSDD) has been proposed (Wang et al. 2006a, b) and has been proved to be effective and robust to deal with neural spike-trains (Liu et al. 2009; Jing et al. 2010a, b)

In the present study, we focused on whether it is possible to discriminate different dynamic natural stimuli by the spatiotemporal activity patterns of a group of synchronized RGCs. The activities of population RGCs in response to digitized time-varying natural images (natural scene movie) were recorded simultaneously from isolated bullfrog retinas using a multi-unit recording system. It was found that the spatiotemporal patterns of the synchronous group RGCs' spike events, which were characterized by MSDD measurements, were more efficient than the temporal patterns of the single cell spike events in discriminating different movie sections. These results suggest that, during natural vision, the local dynamic visual stimuli could be encoded in the dynamic spatiotemporal patterns of the synchronous group RGCs' activities for efficient information transmission.

Methods

Electrophysiology recording

The details of the extracellular-recording procedure have been described in our previous reports (Liu et al. 2007; Jing et al. 2010a, b). All animal experiments were approved by the Ethic Committee, School of Biomedical Engineering, Shanghai Jiao Tong University. All efforts were made to minimize the number of animals used and their sufferings. Briefly, the acutely isolated adult bullfrog retina was immediately transferred onto a piece of multi-electrode array (MEA, MCS GmbH, Germany) with the ganglion cell layer contacting the electrodes. The preparation was super fused with normal oxygenated (95 % O_2 and 5 % CO_2) Ringer's solution (containing in mM: 100.0 NaCl, 2.5 KCl, 1.6 $MgCl_2$, 2.0 $CaCl_2$, 25.0 $NaHCO_3$, 10.0 glucose). Action potentials of RGCs were recorded using a MEA system (8 × 8, MEA60, MCS GmbH, Germany) via a commercial multiplexed data acquisition system with a sampling rate of 20 kHz (MEA, MCS GmbH, Germany). Spikes from individual neurons were sorted using principal component analysis (PCA) (Zhang et al. 2004; Wang et al. 2006b), as well as the spike-detection and spike-sorting procedures provided by the commercial software MC_Rack (Multi Channel Systems MCS GmbH, Germany) and OfflineSorter (Plexon Inc. Texas, USA). Only single-neuron events consistently clarified by all these methods were adopted in further data analyses.

Visual stimulation

Stimuli were generated using programs written in VC ++ and DirectX9 (unless otherwise specified), and displayed on a computer monitor (796 FD II, MAG) and projected onto the isolated retina via a lens system (Zhang et al. 2004). The following stimulation protocols were applied: (1) Pseudo-random checker-board of 4,000 frames, which consisted of 16 × 16 sub-squares, was displayed on the computer monitor at a frame refresh rate of 20 Hz for estimation of the neurons' receptive field properties. Each sub-square was assigned with a value either ''1'' (12.18 nW/cm^2) or ''0'' (0 nW/cm^2) following a pseudo-random binary sequence. (2) A gray scaled natural movie clip constituted by 500 serial frames of natural scenes including trees, sky, roads, etc. This movie clip was selected from a natural movie (VID_A21) in the dataset (van Hateren and Ruderman 1998). The raw data of movie VID_A21 consists of 9,600 frames, of which frames 4,001–4,500 were selected to make up the movie clip used in our experiment reported here. Each frame of the movie clip is consisted of 128 × 128 pixels. The mean photopic intensity of all the pixels of the movie clip was about 3.15 nW/cm^2. The whole length movie clip was displayed at a frame refresh rate of 33.3 Hz (lasted for 15,590 ms) and repeated 20 times in our experiment.

Estimation of the RGCs' receptive fields

The RGCs' receptive fields' properties were estimated by calculating the spike-triggered average (STA) according to

the neuronal responses to the checker-board stimulation described in 2.2 (Meister et al. 1994; Devries and Baylor 1997). The original STA image was then convoluted with a two dimensional spatial Gaussian filters and then converted into a curved surface with two-dimensional interpolation. Finally the receptive field profile was determined by the contour line of the curved surface (Li et al. 2012).

Synchronous group of neurons

Based on the population RGCs' activities in response to the whole-length natural movie (lasted for $L = 15590$ ms, with $R = 20$ repeats), the cross-correlogram between pair-wise neurons was analyzed. For each trial, spike activity of each neuron was symbolized into ''0–1'' sequence (bin size $\Delta t = 1$ ms), where ''1'' represents that there is one spike in the time bin and ''0'' represents that there is no spike in the time bin. Then the spike train was represented by a binary sequence:

$$S_k^r(t) = \begin{cases} 1, & \text{if neuron } k \text{ fired in repetionr,} \\ & \text{during the interval}(t + \Delta t); \\ 0, & \text{otherwise.} \end{cases} \quad (1)$$

The raw cross-correlogram between the target neuron a and the reference neuron k was computed as:

$$C_{ak}(h) = \begin{cases} \sum_{r=1}^{R} \left(\sum_{t=0}^{L-|h|-1} S_a^r(t) S_k^r(t+h)/N \right)/R & h \geq 0, \\ N = \sqrt{\sum_{t=1}^{L} \left(S_a^r(t)\right)^2 \sum_{t=1}^{L} \left(S_k^r(t)\right)^2}; \\ C_{ak}(-h) & h < 0. \end{cases} \quad (2)$$

$C_{ak}(h)$, by definition, represents the correlation between sequences S_a^r and S_k^r with a time lag of h; N is the normalizing factor. A trial-based shift predictor is computed similarly to the cross-correlogram after shifting the target neuron's spike train by one trail relative to that of the reference neuron (Pauluis et al. 2001; Perkel et al. 1967). This procedure is repeated R times ($R = 20$ repeats), and every time shifting the target neuron's spike train by an additional trial. The resulting R correlations are averaged and designated as the trial-based shift predictor. By subtracting the shift predictor from the raw cross-correlogram we get the shift-predicted cross-correlogram, where the co-variation in firing rates of the two cells caused by the light stimulus has been eliminated (Hu et al. 2010). Based on the shift-predicted cross-correlograms, the synchronized pairs were identified as those pairs with the peak value exceeding expected value by 3 standard deviations (Pauluis et al. 2001) and the width of the central peak less than 2 ms. A target RGC together with all its synchronized neighbors was defined as a "synchronous neuron group". We go through every RGC (as a target RGC) of the recorded retinas to identify every possible synchronous neurons group. An example of synchronous neuron group is given in Fig. 1, the target neuron recorded by Channel #24 (Neuron 24) and all its synchronized neighbors (Neuron 12, 15, 23 and 25) composed a synchronous neuron group.

Single cell's temporal firing pattern and the spatiotemporal pattern of group neurons

In the present study, the spike sequences of the synchronous group of G neurons in response to two specific different movie sections (each of which lasted for same time duration $T = 200$ ms) were binned into "0–1" sequences (as described in 2.4, bin size $\triangle t = 1$ ms).

The spatiotemporal patterns of multiple spike events of the group neurons were characterized by MSDD (Fang 1994; Fang et al. 2001). Detailed method was previously reported (Wang et al. 2006a; Jing et al. 2010a). Briefly, for each trial, the k-th neuron' spike event was binned into "0–1" sequences (S_k), and thus the neuronal firing activities were represented by two symbols "0" and "1" ($m = 2$), which are the set elements of $\{0, 1\}$. $S = \{S_1, S_2, \ldots, S_G\}$ represents all the spike sequences of the G member neurons of the group of one trial. In the present study, all the sequences to be analyzed were separated into 6-letter ($l = 6$) overlapping subsequences with moving step being one time bin. Denote the set of all different sequences formed from the set of $\{0, 1\}$ with length l by θ^l. The total number of all sequences of θ^l should be equal to $m^l = 2^6 = 64$. The constructive information of sequence S_k can be represented by its subsequence distribution in θ^l.

The probability distribution of the subsequences in S_k of our data is:

$$U_{S_k}^l = \left\{ p_{k,1}^l, p_{k,2}^l, \ldots, p_{k,64}^l \right\}, \quad (3)$$

where $p_{k,j}$ denotes the probability of subsequence pattern j in sequence k, $\sum_{j=1}^{64} p_{k,j}^l = 1$, $l \ll T$, $k = 1, 2, \ldots, G$.

Given a set of G sequences, we have:

$$\begin{aligned} U_{S_1}^l &= \left\{ p_{1,1}^l, p_{1,2}^l, \ldots, p_{1,64}^l \right\} \\ U_{S_2}^l &= \left\{ p_{2,1}^l, p_{2,2}^l, \ldots, p_{2,64}^l \right\}, \\ &\cdots\cdots \\ U_{S_G}^l &= \left\{ p_{G,1}^l, p_{G,2}^l, \ldots, p_{G,64}^l \right\} \end{aligned} \quad (4)$$

Then the B_k value for the k-th sequence can be calculated as:

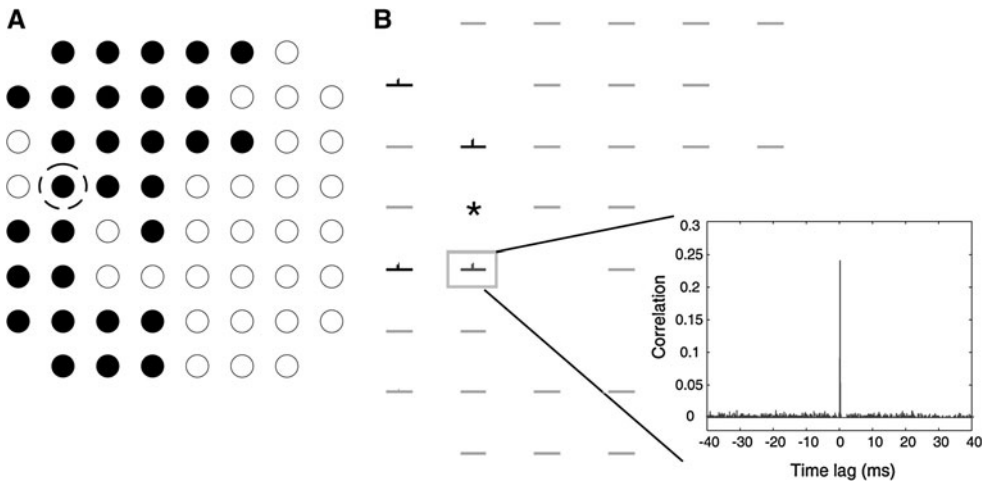

Fig. 1 **a** Positions of the electrodes by which 30 RGCs of the example retina were recorded (indicated by the *filled circles*). An example of "target cell" is indicated by the dashed circle. **b** Shift-predicted cross-correlograms of the target cell (indicated by the *black asterisk*) paired with other 29 cells, whose electrode positions are indicated in (**a**). Synchronous activities were found between the target cell and 4 of its neighboring cells (*black traces*). Thus the synchronous group consists of 5 RGCs. The gray plots show neuron pairs with no significant synchronous activities

$$B_k\left(U^l_{s_1},\ U^l_{s_2},\ldots,U^l_{s_G}\right)=\sum_{j=1}^{64}p^l_{k,j}\log\frac{p^l_{k,j}}{\sum_{k=1}^{G}p^l_{k,j}\Big/G}, \qquad (5)$$

Therefore, if the two sequences S_i and S_j $(i\neq j,\ i,j\leq G)$ have the same subsequence distribution $U^l_{S_i}=U^l_{S_j}$, we should have the result of $B_i\left(U^l_{s_1},U^l_{s_2},\ldots,U^l_{s_G}\right)=B_j\left(U^l_{s_1},U^l_{s_2},\ldots,U^l_{s_G}\right)$. It implies that if two spike trains are completely synchronized, they will have exactly the same B_k values, and a large B_k value is related to profound difference between the temporal structure of the k-th sequence and the rest of the group.

Thus the spatiotemporal pattern of the spike events of the group of G neurons in response to a specific movie section of a given trial could be represented by $W=(B_1,\ B_2,\ldots,B_G)$.

Classification analysis

To assess the performance of the RGCs in discriminating different brief sections of the natural movie, classification analyses based on single cell and population neuronal activities were performed respectively. In this paper, each trial of single cell firing pattern (S_k) was presented as a point in a T-dimensional space ($T=200$ is the length of S_k). Whereas the B_k values of group neurons (W) estimated by MSDD method (which was presented as a point in a G-dimensional space, details in 2.5) was applied to represent the spatiotemporal pattern of the synchronous group. The classification procedure is aimed to assign these data points into different clusters corresponding to the different movie sections.

In the present study, Support Vector Machines (SVMs) method was used to discriminate the neuronal activities in response to the two different movie sections as represented by the data clusters in the n-dimensional space. SVMs separate the different classes of data by a hyper-plane. An optimal separation is achieved by the maximal margin hyper-plane (Furey et al. 2000). They can work in combination with the technique of 'kernels' that automatically realizes a non-linear mapping to a feature space to deal with the linear non-separable cases (Furey et al. 2000; Noble 2006). SVMs classifier used in the present study is a freely available toolbox with implements for support vector machines based on libsvm, 2009 (Software available at http://www.ilovematlab.cn), which is a modified version of Chih-Chung Chang and Chih-Jen Lin's LIBSVM: a library for support vector machines, 2001 (Software available at http://www.csie.ntu.edu.tw/∼cjlin/libsvm).

The procedure of classifying the neuronal responses to two distinct patterns consisted of two steps: (1) Performing the hold-out cross-validation experiment. To build up the "training-data", 15 trials out of all the 20 trails of neuronal responses to the two distinct movie sections were randomly chosen, and the remaining 5 trials of neuronal responses were used as test-data. (2) Training the SVM classifier with the training data to work out the maximal margin hyper-plane that separates the neuronal responses to the two movie sections into two classes. Then the test-data were classified by the trained classifier (the hyper-plane), and the ratio of the correctly labeled trials (the number of correct ones/5) was calculated. In this paper, in classifying the single cell temporal firing patterns (Sk) or the population neuronal spatiotemporal patterns (W) in response to two

distinct movie sections, the classification procedures (1) and (2) described above were repeated 10 times independently, and the training-data set was chosen randomly for each time. The averaged value of the correct ratio was determined as the discrimination accuracy of the neuronal responses to the two distinct movie sections.

Results

Population neuronal activities of two retinas in response to the pseudo-random checker-board flickering and natural movie stimulation were recorded (details in 2.2). In total 15 synchronous neuron groups from retina 1 and 9 from retina 2 were identified according to methods in 2.4. The whole natural movie stimulation lasted for 15.59 s and repeated 20 times. We found that in response to some sections of the natural movie, synchronous group of RGCs fired with similar spike trains. How could synchronized neurons in a group discriminate the different movie sections through such similar spike trains? We aim to examine the role of the synchronous activities of RGCs in discriminating different movie sections in the present study. For each identified synchronous neuron group during the whole natural movie stimulation in the present study, we picked out their spike trains that showed similar responsive patterns to two movie sections. These movie section pairs are not of the same for different synchronous neuron groups. Taking one synchronous group including Neuron 12, 15, 23, 24 and 25 from retina 1 (as described in 2.4), for example, the firing properties of the neuronal activities and their contributions to movie section discrimination are described in the following text .

Single cell receptive field profiles and the movie sections

Based on the neuronal responses to the checker-board flickering, each neuron's receptive field property was estimated by calculating the spike-triggered average (STA). Figure 2a gives the receptive field profiles of every single neuron from the synchronous neuron group presented in Fig. 1, showing that the receptive fields of the neurons in the group overlapped with each other. We also found overlapped receptive fields of neurons in other synchronous neuron groups.

The image patches of the two movie sections, which evoked similar spike events of the example synchronous neuron group are shown in Fig. 2b and c. Each movie section contains three successive frames. The two movie sections are similar in light intensity, contrast and spatial

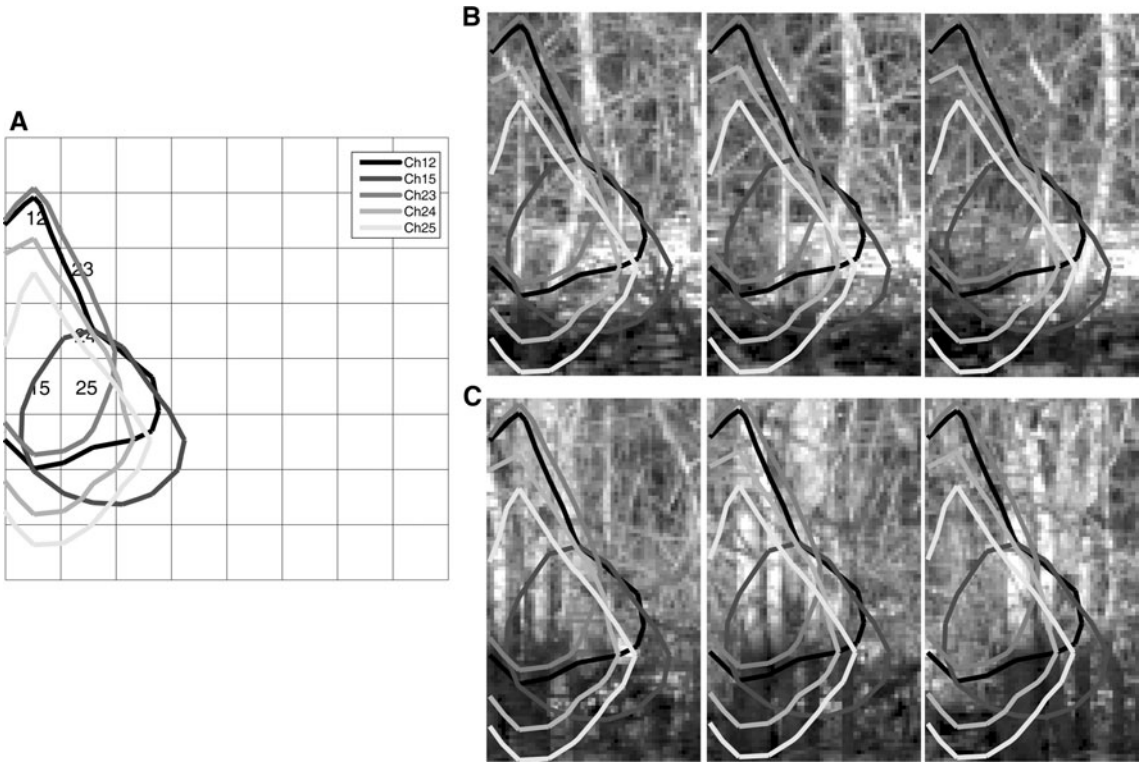

Fig. 2 Single cell receptive field profiles and the image patches of two distinct movie sections. **a** Geometric positions of the electrodes by which the single cell activities of the example synchronous group neurons were recorded and the receptive field profile of each recorded neuron (indicated by different gray scale curves). **b** and **c** Successive image patches of the two movie sections imposed on each group neuron's receptive field

structure of the scenes. Movie section pairs for other synchronous neuron groups also had similar light intensity, contrast and spatial structure of the scenes.

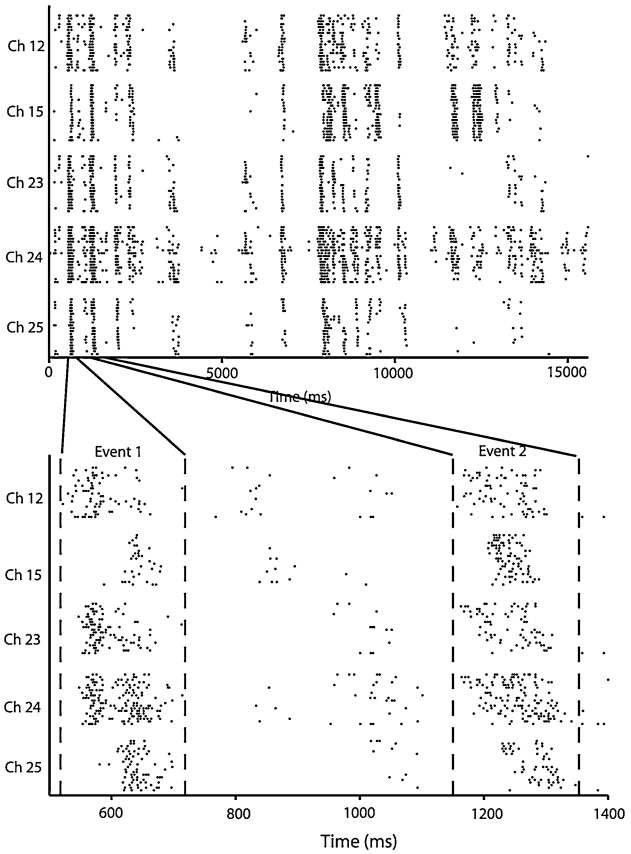

Fig. 3 Spike trains and spike events of the synchronous group neurons' activities. The *top* panel shows the group neurons' activities in response to the whole-length natural movie stimulation (each dot represent one spike fired at that moment). The *bottom* panel shows the enlarged spike events of the group neurons elicited by two distinct movie sections in Fig. 2 (the paired *dash lines* indicate the start and end time of the spike event)

Individual RGCs' spike events in response to different movie sections

Figure 3 showed the activities of a group of synchronized neurons presented in Fig. 1 to the two movie sections (as shown in Fig. 2b and c). These neuron's spike events in response to two movie sections were denoted as Event 1 and Event 2 (each lasted for 200 ms), respectively. The two spike events show general similarity in duration and overall firing counts. However, the enlarged details in the bottom panel of Fig. 3 show that individual neurons' activity as well as the relative timing of the neurons' activities in Events 1 and 2 was different.

We first examined each neuron's mean firing rates during Events 1 and 2 (Fig. 4a). It is shown that for most neurons (Neuron 12, 23, 24 and 25), the mean firing rates over the 200-ms duration were similar for different Events (paired t test, $p > 0.05$). However, the PSTHs of individual neurons show obvious difference during their responses to the two movie sections (shown in Fig. 4b and c, time bin = 5 ms, averaged over 20 trials). These results suggest that it is hardly to distinguish different movie sections by the differences of the single cell mean firing rates over the duration of the events, but the different temporal structure of each individual neurons' activities as well as the different relative timing of group neurons' activities in Event 1 and Event 2 may provide some clues for discriminating the movie sections.

Classification of the neuronal activities in response to different movie sections

In response to the different movie sections, both the individual neuron's temporal firing pattern as defined in Eq. 1 (S_k for the k-th neuron, $k = 1, 2, \ldots, G$) and the group neurons' spatiotemporal firing patterns (W, the vector of the group neurons' B_k values, $k = 1, 2, \ldots, G$) (detail

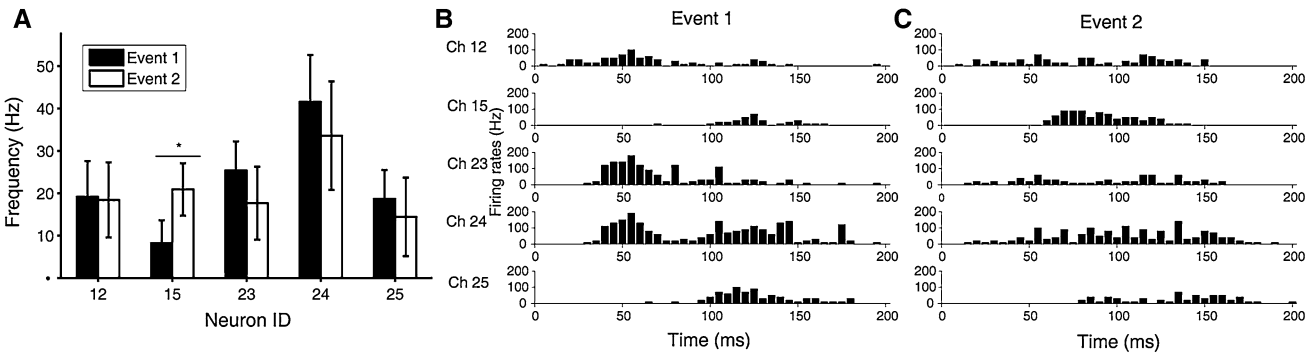

Fig. 4 Individual neurons' mean firing rates in response to the two different movie sections. **a** Each *bar* represents one neuron's mean firing rate averaged over 20 trials in response to one movie section, the *error bar* represents the standard deviation. "*" indicates significant difference between each individual neuron's activities in Event 1 and Event 2. **b** and **c** PSTH of individual neurons' firing events in response to different movie sections

procedures see 2.5) are different. SVM method was used to classify the neuronal firing patterns in response to different movie sections.

It is shown in Fig. 4b that there are obvious difference between the PSTHs of individual neurons' Event 1 and Event 2, which suggests that the discrimination of the movie sections could be based on the individual neurons' temporal firing patterns. Furthermore, as visualized in Fig. 5, the group neurons' spatiotemporal firing patterns in Event 1 and Event 2, which was characterized by the group neurons' B_k values, are highly distinguishable. Although situations varied across trials, the general trend of the difference between the spatiotemporal firing patterns of Event 1 and Event 2 were consistent. As shown in Fig. 6a, this is confirmed by the classification accuracy of the group neuronal spatiotemporal patterns (82 % ± 3.89 %, mean ± SE), which obviously exceed the mean classification accuracy of the single neuronal temporal firing patterns (70 % ± 4.06 %, mean ± SE) (unpaired t test, $p < 0.05$).

We next examined the overall performance of the synchronous neuron groups. The neuronal activities of 24 synchronous neuron groups (including 51 neurons altogether) from two retinas in response to different movie section pairs (an example is given in Fig. 2) were taken to do the classification analysis. It is shown in Fig. 6b that the mean classification accuracy of the single neuronal temporal firing patterns was 57 % ± 7.06 % (mean ± SE), while that of the group neuronal spatiotemporal patterns was 79 % ± 3.89 % (mean ± SE). It is conspicuous that the group neuronal spatiotemporal patterns outperformed the single neuronal temporal firing patterns in discriminating different movie sections (unpaired t test, $p < 0.05$).

All the results reveal that during natural movie stimulation, different movie sections elicited spike events with both different temporal firing patterns of single neurons and different spatiotemporal firing patterns of synchronous neuron groups; however the group neuronal spatiotemporal patterns were more reliable for discriminating the movie sections. It is suggested that the tiny local changes of the

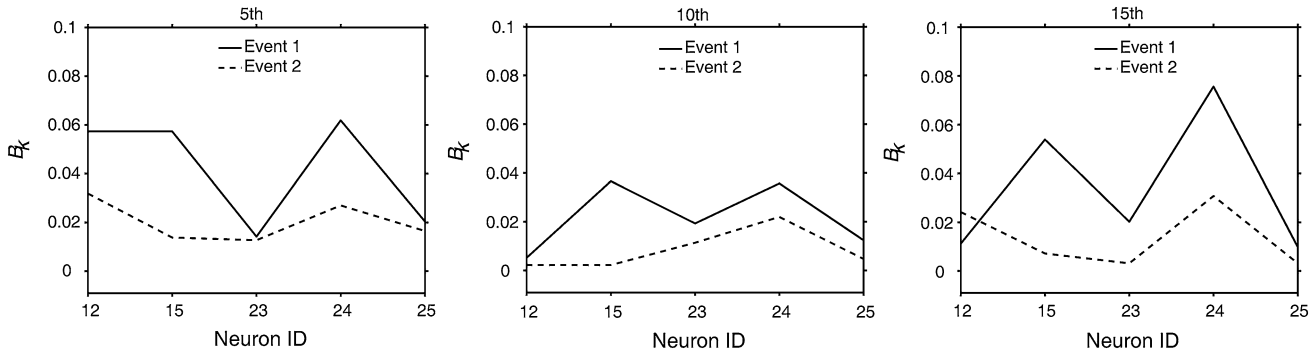

Fig. 5 B_k values of the example 5 synchronous neurons' activities in Event 1 and Event 2 of 5th (*left panel*), 10th (*middle panel*) and 15th (*right panel*) trials in response to the natural movie stimulation

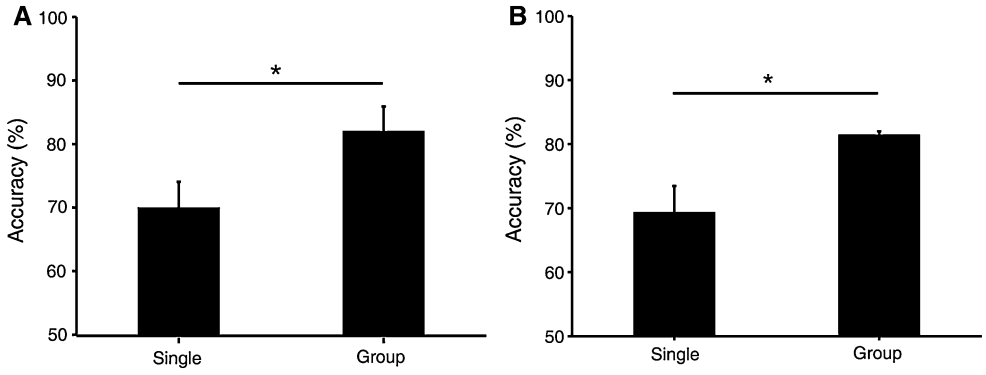

Fig. 6 SVM classification accuracy. **a** The mean classification accuracy of the single neurons' temporal firing patterns (5 neurons from the example group) and the group neurons' spatiotemporal firing patterns are denoted by the bars. Error bars represent SE. Significant difference (based on unpaired t test) is marked by *asterisks* (*, $p < 0.05$). **b**The mean classification accuracy of all the single neuronal temporal firing pattern pairs ($N = 68$) and the group neurons' spatiotemporal firing patterns (24 groups from two retinas) are denoted by the bars. *Error bars* represent SE. Significant difference (based on unpaired t test) is marked by *asterisks* (*, $p < 0.05$)

natural movie frames can be encoded by the synchronous neurons' spatiotemporal patterns and transmitted efficiently to the target neurons.

Discussions

Sensory systems are believed to convey information about the environment to the brain using a population code (Rieke et al. 1997; Schneidman et al. 2003; Latham and Nirenberg 2005; Qu et al. 2012). Previous studies showed that RGCs often fire in a synchronizing way, suggesting that synchronized firing patterns could be important for neuronal population code (Schnitzer and Meister 2003; Schneidman et al. 2006; Shlens et al. 2009). However, during natural movie stimulation, the synchronous neurons, may fire in similar spike events in response to different movie sections (as shown in Fig. 3). It is intriguing that how the target neurons recognize the different movie sections via similar synchronized activities.

In this paper, the performances of the individual neuronal temporal firing patterns and the group neuronal spatiotemporal patterns in the movie section discrimination are investigated. The results reveal that during natural vision, neuron groups exhibited higher classification accuracy in movie section discrimination than single cells (Fig. 6). The synchronization strength is not equally distributed across the neuronal subsets and varies with the stimulus pattern that covers the mosaic of multi-neuronal receptive fields when exposed to visual stimulations (Neuenschwander and Singer 1996). The alterable and dynamic synchronization of neuron groups empowers the neurons to have an extended information coding capacity to indentify the difference between the stimulation patterns. These are consistent with the notion that correlation among neuron population activities improves the neural coding efficiency and information transmission (Pillow et al. 2008; Koch et al. 2004; Schnitzer and Meister 2003; Liu et al. 2011).

Measurement based on subsequence distribution discrepancy method was used to characterize the spatiotemporal patterns of the group neurons' activities, which makes the spatiotemporal pattern differences between the population neurons' activities in response to the two movie sections be clearly eyeballed (Fig. 6). The high classification accuracy of the group neurons' spatiotemporal patterns in Event 1 and Event 2 reflected that the differences in the population activity patterns were consistently detectable during repeated experimental trials. MSDD method is efficient in characterizing the spatiotemporal patterns of the population neuronal activities.

In summary, neuronal pattern discrimination in the present study indicates that population activity promotes the performance in discrimination. The dynamic visual stimuli could be encoded in the dynamic spatiotemporal patterns of the synchronous group RGCs' activities for efficient information transmission, whereas the temporal patterns of individual neuronal activities are inadequate for representing the complex and dynamic natural stimuli. The specific spatiotemporal activity patterns of the synchronized activities may convey different information of the stimuli and be suggested as a special symbol in the population code.

Acknowledgments This work was supported by the grant from National Foundation of Natural Science of China (No. 11232005 and No. 61075108). The authors thank Xin-Wei Gong and Hao Li from School of Biomedical Engineering at Shanghai Jiao Tong University for important technical contributions and informative discussions.

References

Brivanlou IH, Warland DK, Meister M (1998) Mechanisms of concerted firing among retinal ganglion cells. Neuron 20:527–539

Carandini M, Demb JB, Mante V, Tolhurst DJ, Dan Y, Olshausen BA, Gallant JL, Rust NC (2005) Do we know what the early visual system does? J Neurosci: Off J Soc Neurosci 25: 10577–10597

Devries SH, Baylor DA (1997) Mosaic arrangement of ganglion cell receptive fields in rabbit retina. J Neurophysiol 78:2048–2060

Du Y, Wang RB, Han F, Lu QS (2012) Firing pattern and synchronization property analysis in a network model of the olfactory bulb. Cogn Neurodyn 6(2):203–209

Einhauser W, Konig P (2010) Getting real-sensory processing of natural stimuli. Curr Opin Neurobiol 20:389–395

Endeman D, Kamermans M (2010) Cones perform a non-linear transformation on natural stimuli. J Physiol 588:435–446

Fang WW (1994) Disagreement degree of multi-person judgements in an additive structure. Math Soc Sci 28:85–111

Fang WW, Roberts FS, Ma ZR (2001) A measure of discrepancy of multiple sequences. Inf Sci 137:75–102

Felsen G, Dan Y (2005) A natural approach to studying vision. Nat Neurosci 8:1643–1646

Furey TS, Cristianini N, Duffy N, Bednarski DW, Schummer M, Haussler D (2000) Support vector machine classification and validation of cancer tissue samples using microarray expression data. Bioinformatics 16:906–914

Geisler WS (2008) Visual perception and the statistical properties of natural scenes. Annu Rev Psychol 59:167–192

Gerstein GL, Aertsen AM (1985) Representation of cooperative firing activity among simultaneously recorded neurons. J Neurophysiol 54:1513–1528

Gong HY, Zhang YY, Liang PJ, Zhang PM (2010) Neural coding properties based on spike timing and pattern correlation of retinal ganglion cells. Cogn Neurodyn 4:337–346

Hu EH, Pan F, Volgyi B, Bloomfield SA (2010) Light increases the gap junctional coupling of retinal ganglion cells. J Physiol 588:4145–4163

Jing W, Liu WZ, Gong XW, Gong HQ, Liang PJ (2010a) Influence of GABAergic inhibition on concerted activity between the ganglion cells. Neuro Rep 21:797–801

Jing W, Liu WZ, Gong XW, Gong HQ, Liang PJ (2010b) Visual pattern recognition based on spatio-temporal patterns of retinal ganglion cells' activities. Cogn Neurodyn 4:179–188

Koch K, McLean J, Berry M, Sterling P, Balasubramanian V, Freed MA (2004) Efficiency of information transmission by retinal ganglion cells. Curr Biol 14:1523–1530

Konig P (1994) A method for the quantification of synchrony and oscillatory properties of neuronal activity. J Neurosci Methods 54:31–37

Kreuz T, Haas JS, Morelli A, Abarbanel HD, Politi A (2007) Measuring spike train synchrony. J Neurosci Methods 165: 151–161

Latham PE, Nirenberg S (2005) Synergy, redundancy, and independence in population codes, revisited. J Neurosci: Off J Soc Neurosci 25:5195–5206

Lesica NA, Ishii T, Stanley GB, Hosoya T (2008) Estimating receptive fields from responses to natural stimuli with asymmetric intensity distributions. PLoS One 3:e3060

Li H, Liu WZ, Liang PJ (2012) Adaptation-dependent synchronous activity contributes to receptive field size change of bullfrog retinal ganglion cell. PLoS One 7:e34336

Liu X, Zhou Y, Gong HQ, Liang PJ (2007) Contribution of the GABAergic pathway(s) to the correlated activities of chicken retinal ganglion cells. Brain Res 1177:37–46

Liu X, Li H, Liang PJ (2009) Estimation of concerted activities based on subsequence distribution discrepancy calculation. The 3rd IEEE Internationl Conference on Bioinformotic and Biomedical Engineering. pp 1–3

Liu WZ, Yan RJ, Jing W, Gong HQ, Liang PJ (2011) Spikes with short inter-spikeintervals in frog retinal ganglion cells are more correlated with their adjacent neurons' activities. Protein Cell 2:764

Mante V, Bonin V, Carandini M (2008) Functional mechanisms shaping lateral geniculate responses to artificial and natural stimuli. Neuron 58:625–638

Meister M (1996) Multineuronal codes in retinal signaling. Proc Natl Acad Sci USA 93:609–614

Meister M, Pine J, Baylor DA (1994) Multi-neuronal signals from the retina: acquisition and analysis. J Neurosci Methods 51:95–106

Meister M, Lagnado L, Baylor DA (1995) Concerted signaling by retinal ganglion cells. Science 270:1207–1210

Neuenschwander S, Singer W (1996) Long-range synchronization of oscillatory light responses in the cat retina and lateral geniculate nucleus. Nature 379:728–732

Noble WS (2006) What is a support vector machine? Nat Biotechnol 24:1565–1567

Pauluis Q, Baker SN, Olivier E (2001) Precise burst synchrony in the superior colliculus of the awake cat during moving stimulus presentation. J Neurosci: Off J Soc Neurosci 21:615–627

Perkel DH, Gerstein GL, Moore GP (1967) Neuronal spike trains and stochastic point processes. II. Simultaneous spike trains. Biophys J 7:419–440

Pillow JW, Shlens J, Paninski L, Sher A, Litke AM, Chichilnisky EJ, Simoncelli EP (2008) Spatio-temporal correlations and visual signalling in a complete neuronal population. Nature 454:995–999

Qu JY, Wang RB, Du Y (2012) Synchronization study in ring-like and grid-like neuronal networks. Cogn Neurodyn 6(1):21–31

Reinagel P (2001) How do visual neurons respond in the real world? Curr Opin Neurobiol 11:437–442

Rieke F, Warland D, de Ruyter van Steveninck R, Bialek W (1997) Spikes: exploring the neural code MIT Press

Rust NC, Movshon JA (2005) In praise of artifice. Nat Neurosci 8:1647–1650

Schneidman E, Bialek W, Berry MJ 2nd (2003) Synergy, redundancy, and independence in population codes. J Neurosci: Off J Soc Neurosci 23:11539–11553

Schneidman E, Berry MJ 2nd, Segev R, Bialek W (2006) Weak pairwise correlations imply strongly correlated network states in a neural population. Nature 440:1007–1012

Schnitzer MJ, Meister M (2003) Multineuronal firing patterns in the signal from eye to brain. Neuron 37:499–511

Shlens J, Field GD, Gauthier JL, Grivich MI, Petrusca D, Sher A, Litke AM, Chichilnisky EJ (2006) The structure of multi-neuron firing patterns in primate retina. J Neurosci: Off J Soc Neurosci 26:8254–8266

Shlens J, Field GD, Gauthier JL, Greschner M, Sher A, Litke AM, Chichilnisky EJ (2009) The structure of large-scale synchronized firing in primate retina. J Neurosci: Off J Soc Neurosci 29: 5022–5031

Talebi V, Baker CL Jr (2012) Natural versus synthetic stimuli for estimating receptive field models: a comparison of predictive robustness. J Neurosci: Off J Soc Neurosci 32:1560–1576

van Hateren JH, Ruderman DL (1998) Independent component analysis of natural image sequences yields spatio-temporal filters similar to simple cells in primary visual cortex. Proc Biol Sci/ Royal Soc 265:2315–2320

Wang GL, Liu X, Zhang PM, Liang PJ (2006a) A new method for multiple spike train analysis based on information discrepancy. LNCS 4232:30–38

Wang GL, Zhou Y, Chen AH, Zhang PM, Liang PJ (2006b) A robust method for spike sorting with automatic overlap decomposition. IEEE Trans Biomed Eng 53:1195–1198

Zhang PM, Wu JY, Zhou Y, Liang PJ, Yuan JQ (2004) Spike sorting based on automatic template reconstruction with a partial solution to the overlapping problem. J Neurosci Methods 135:55–65